Self-tuning of threshold for a two-state system

Boyoung Seo,[1] Raishma Krishnan,[2] and Toyonori Munakata[1,*]
[1]*Department of Applied Mathematics and Physics, Graduate School of Informatics, Kyoto University, Kyoto 606-8501, Japan*
[2]*Institute of Physics, Sachivalaya Marg, Bhubaneswar 751005, Orissa, India*
(Received 27 February 2007; published 9 May 2007)

A two-state system (TSS) under time-periodic perturbations (to be regarded as input signals) is studied in connection with self-tuning (ST) of threshold and stochastic resonance (SR). By ST, we observe an improvement of the signal-to-noise ratio (SNR) in a weak-noise region. An analytic approach to a tuning equation reveals that SNR improvement is possible also for the large-noise region and this is demonstrated by Monte Carlo simulations of hopping processes in a TSS. ST and SR are discussed from a little more physical point of view of the energy transfer (dissipation) rate, which behaves in a similar way as the SNR. Finally ST is considered briefly for a double-well potential system, which is closely related to the TSS.

DOI: 10.1103/PhysRevE.75.056106 PACS number(s): 05.10.Gg, 02.70.Uu, 05.40.−a

I. INTRODUCTION

Recently the constructive or beneficial roles of noise have gathered considerable interest in many fields, such as physical [1] and biological [2] sciences as well as engineering [3]. One of the conspicuous effects of noise or random disturbance is that it can drive a dynamical system out of an equilibrium state, thus giving a lifetime or Kramers time [4] to (metastable) equilibrium states.

The simulated annealing method [3], which is used to search for solutions to minimization (or more generally optimization) problems in a complex system, employs noise to prevent a search process from being trapped in local minimum (metastable) states. Sophisticated algorithms are developed to efficiently escape from local metastable states, which are useful for both simulated annealing and efficient Monte Carlo simulations [5].

Stochastic resonance (SR) [1] is a phenomenon in which information transfer from input to output signals can be significantly increased by noise with appropriate (nonzero) intensity. One can comprehend SR by considering a simple threshold system [6], which gives 1 (0) as an output signal x if input signal s plus noise ξ is larger (smaller) than a certain threshold value a. If an input signal s is always smaller than a and there is no noise, x is always equal to 0 and information transfer through the threshold system is impossible. By adding noise ξ to s, there is some possibility of $s+\xi>a$, producing $x=1$ and information about s is conveyed through the threshold system. However, large noise deforms the original input signals too much, leading to no correlation between s and x, resulting in no information transfer from input to output signals.

As a system similar to the threshold system mentioned above, let us consider an overdamped Brownian particle in a double-well potential driven by a sinusoidal time-periodic force, which was proposed and studied as a model for Earth's ice ages [7]. This model has an activation energy and Gaussian Brownian noise ξ_G, which may be regarded as the threshold value a and the noise ξ, respectively, in the threshold system. In this case information on input signal, such as the frequency $2\pi\omega_0$ of the sinusoidal force, is transferred as the peak position in the power spectrum of the output signal. When the variance (or temperature from the fluctuation-dissipation theorem) of ξ_G is tuned to an appropriate value, which turns out to be nonzero, the signal-to-noise ratio (SNR) attains its maximum value.

From this we may consider that SR has a close relation with synchronization, especially when the external disturbance is characterized by a frequency $f_0=2\pi\omega_0$. In this regard we mention stochastic synchronization, in which an excitable system, like neurons, responds in synchrony with a external disturbance (signal), which has also gathered lots of interest in connection with electroreceptors in the paddlefish [8].

When input signals are subthreshold, the ability of a threshold system to transfer information is considerably limited for weak noise, as mentioned above. To improve information transfer in this region, we proposed recently a simple adaptation process [9] for a threshold value a hinted at by a self-tuning mechanism proposed to explain auditory sensitivity [10] when the input signal becomes very weak.

In this paper we consider effects of self-tuning (ST) of the threshold value for a two-state system (TSS) driven by a sinusoidal signal. One merit of the TSS is that one can calculate the SNR accurately [11] by solving a differential equation, without doing numerical experiments to obtain the power spectrum, based on which the SNR is usually calculated. In Sec. II we introduce our system, the TSS, and a closely related double-well potential system (DWPS) and propose a mechanism to control a threshold value—i.e., the activation energy. In Sec. III numerical results for the SNR, the probability density for residence time [12], stochastic dynamics of threshold values, and the firing rate for the TSS are presented. We show that a large SNR is achieved in the small-noise region as expected. In Sec. IV the adaptation process, which is governed by a threshold equation with two parameters α and β, is studied both analytically and numerically. We discuss how these parameters affect the quality of information transfer, with the main emphasis put on the large-noise region. The final section contains some comments on the energy transfer rate from input signals to a reservoir and on the DWPS.

*Electronic address: munakata@amp.i.kyoto-u.ac.jp

II. MODEL

In this section we first introduce the TSS [11] and relate it to the DWPS for convenience for later discussions on the physical aspects of the model such as energy transfer to a reservoir. The system variable $x(t)$ at time t is assumed to take only two values $x_+=1$ and $x_-=-1$, and the transition between the two states is described by the master equation

$$dp_+(t)/dt = -w_-(t)p_+(t) + w_+(t)[1-p_+(t)], \tag{1}$$

where $p_+(t)$ denotes the probability that $x(t)=x_+$ with $p_+(t)+p_-(t)=1$. $w_-(t)$ is the transition probability at time t for the particle to jump to the left(x_-) site and $w_+(t)$ is similarly defined.

The rates $w_+(t)$ and $w_-(t)$ are expressed in an Arrhenius form as

$$w_+(t) = \exp\{[-a + A_0\cos(\omega_0 t)]/T\},$$

$$w_-(t) = \exp\{[-a - A_0\cos(\omega_0 t)]/T\}, \tag{2}$$

where T measures strength of noise and $a \pm A_0\cos(\omega_0 t)$ denotes (time-dependent) activation energy for jumping.

A physical system which is closely related to the TSS is the DWPS described by the Langevin equation

$$dx/dt = -dV(x)/dx + A_0\cos(\omega_0 t) + f(t), \tag{3}$$

where the random force $f(t)$ satisfies the fluctuation-dissipation relation

$$\langle f(t)f(t')\rangle = 2T\delta(t-t') \tag{4}$$

and $V(x)$ represents the double-well potential:

$$V(x) = a(x-1)^2(x+1)^2. \tag{5}$$

When both A_0 and T are smaller than a in Eq. (5), the Brownian particle described by Eq. (3) may be considered to stay either at $x_+=1$ or $x_-=-1$ for time of the order of Kramers time $\tau_{Kr} \simeq \exp(a/T)$ [4] and occasionally jumps between x_+ and x_-.

When the relaxation time $\tau_r \simeq (8a)^{-1}$ of intrawell motion is short in the sense $\tau_r\omega_0 \ll 1$ one can introduce the adiabatic assumption to reduce the DWPS approximately to the TSS described by Eq. (1).

Both the TSS and DWPS are extensively studied in connection with SR and are known to show SR [1]; that is, SNR shows a maximum at nonzero T when other parameters characterizing the system, such as activation energy a and ω_0, A_0, are kept fixed. It may be noted that for the TSS [11,12] analytic (or integral form) results for the SNR and the distribution function $p_{fp}(\tau)$ of the first passage time for jumping to another state are available. One merit of the TSS is that even if we take effects of ST into account, we can calculate the SNR by solving a coupled set of differential equations (1) and (6), to be given below, without recourse to Monte Carlo simulations, which inevitably introduce fluctuations to power spectra and consequently to the SNR.

Here we introduce a mechanism for ST of the activation energy a in Eqs. (2), following the prescription presented in Ref. [9]. If there occurs no jumping or activation events, $a(t)$ simply decreases, while if a jumping event occurs, $a(t)$ increases, thus controlling the jumping or firing rate by avoiding too large or too small firing rates. To express this adaptation process mathematically, we employ the following dynamics for $a(t)$:

$$da(t)/dt = -\alpha a(t) + \beta[w_+(t)p_-(t) + w_-(t)p_+(t)]. \tag{6}$$

Indeed, if we tentatively put $\beta=0$, $a(t)$ goes to zero since α is chosen to be positive. If we put β positive, we notice that $a(t)$ increases in proportion to the barrier crossing rate. By this mechanism we expect that the TSS adjusts $a(t)$, reflecting the circumstances it is put in.

For the DWPS we propose a similar adaptation dynamics for $a(t)$ of the form

$$da(t) \equiv a(t+dt) - a(t) = -\alpha a(t)dt + \beta\int_t^{t+dt} d\tau \Sigma_i \delta(t-t_i), \tag{7}$$

where t_i $(i=1,2,\ldots)$ denotes the time when $x(t)=1$.

III. NUMERICAL RESULTS FOR THE TSS

We first explain how one can calculate the SNR for the TSS with ST, by slightly modifying the approach in Ref. [11].

A. SNR with self-tuning: Methodology

Let us denote the solution to Eqs. (1) and (6) as

$$p_+(t) = p_+(t|x_0,a_0,t_0), \quad a(t) = a(t|x_0,a_0,t_0), \tag{8}$$

which satisfy the initial conditions $p_+(t=t_0|x_0,a_0,t_0) = \delta(1,x_0)$ and $a(t=t_0|x_0,a_0,t_0)=a_0$ with $\delta(1,x)$ denoting the Kronecker δ—i.e., $\delta(1,x)=1$ if $x=1$ and $\delta(1,x)=0$ if $x\neq 1$. The transition probability $p(x,a,t|x_0,a_0,t_0)$ for $(x(t),a(t))$ to be at (x,a) starting from (x_0,a_0) is expressed as

$$p(x,a,t|x_0,a_0,t_0) = \delta(a-a(t|x_0,a_0,t_0))\{p_+(t|x_0,a_0,t_0)\delta(x-1) + [1-p_+(t|x_0,a_0,t_0)]\delta(x+1)\}. \tag{9}$$

Following MacNamara and Wiesenfeld [11] let us first introduce the time correlation function $\phi(t,\tau|x_0,a_0,t_0)$ by

$$\phi(t,\tau|x_0,a_0,t_0) = \langle x(t)x(t+\tau)|\ x_0,a_0,t_0)\rangle \equiv \int da' \int da \int dx \int dy x y p(x,a',t+\tau|y,a,t)p(y,a,t|x_0,a_0,t_0). \tag{10}$$

After performing integration of Eq. (10) over y and a we have

$$\phi(t,\tau|x_0,a_0,t_0) = \int da' \int dx x[p_+(t|x_0,a_0,t_0) \times p(x,a',t+\tau|1,a(t|x_0,a_0,t_0),t) - p_-(t|x_0,a_0,t_0) \times p(x,a',t+\tau|-1,a(t|x_0,a_0,t_0),t)]. \tag{11}$$

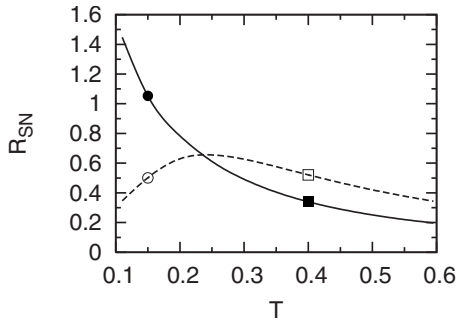

FIG. 1. SNR (R_{SN}) as a function of noise intensity T for system with (solid curve) and without (dashed curve) ST. For ST we use $\alpha=0.03$ and $\beta=0.1$ in Eq. (6). The barrier height is set $a=0.5$ for the system without ST. Here and hereafter ω_0 and A_0 are always set to be $\omega_0=0.5$ and $A_0=0.3$.

Now we take the limit $t_0\to-\infty$ to remove the x_0, a_0 dependence of p_+, p_- and of a on the right-hand side of Eq. (11), leading to

$$\phi(t,\tau)=\int da'\int dxx[p_+(t)p(x,a',t+\tau|1,a(t),t) - p_-(t)p(x,a',t+\tau|-1,a(t),t)], \quad (12)$$

where we replace $\lim_{t_0\to-\infty}p_+(t|x_0,a_0,t_0)$ by $p_+(t)$ and $\lim_{t_0\to-\infty}a(t|x_0,a_0,t_0)$ by $a(t)$. $\int da'$ can be performed trivially to have

$$\phi(t,\tau)=p_+(t)[2p_+(t+\tau|1,a(t),t)-1] - p_-(t)[2p_+(t+\tau|-1,a(t),t)-1]. \quad (13)$$

Finally to make the function $\phi(t,\tau)$ independent of the time variable t and also to conform to experimental situations, we take time average $(1/\tau_p)\int_0^{\tau_p}dt$ with $\tau_p=2\pi/\omega_0$ to obtain

$$\phi(\tau)=(1/\tau_p)\int_0^{\tau_p}dt\{p_+(t)[2p_+(t+\tau|1,a(t),t)-1] - p_-(t)[2p_+(t+\tau|-1,a(t),t)-1\ \}. \quad (14)$$

Numerical implementation of Eq. (14) is not difficult, and the result is conveniently expressed as

$$\phi(\tau)\approx\phi_{relax}(\tau)+B\cos(\omega_0\tau), \quad (15)$$

where $\phi_{relax}(\tau)$ is the relaxation part, which goes to zero asymptotically as $\tau\to\infty$, and $B\cos(\omega_0\tau)$ represents the periodic part of the external field. Fourier transformation of Eq. (15) has the form

$$\tilde{\phi}(\omega)=\tilde{\phi}_{relax}(\omega)+B[\delta(\omega-\omega_0)+\delta(\omega_0+\omega_0)], \quad (16)$$

and the SNR is defined here as

$$R_{SN}=B/\tilde{\phi}_{relax}(\omega_0). \quad (17)$$

B. Numerical results for the SNR and other quantities

It is noted that we take $\omega_0=0.5$ and $A_0=0.3$ in the following. In Fig. 1 is plotted the SNR for systems with self-tuning ($\alpha=0.03$ and $\beta=0.1$, $C\equiv\alpha/\beta=0.3$) and without self-tuning ($a=0.5$). We observe that the SNR is improved by self-tuning in the low-temperature region. This is confirmed from the first-passage time distribution function $p_{fp}(\tau)$ shown in Fig. 2 for the two systems marked by a black circle with ST and by a white circle (without ST) in Fig. 1 ($T=0.15$). These $p_{fp}(\tau)$ are obtained by Monte Carlo simulations, in which we actually followed particle motion with the hopping rate given by Eq. (2) and obtained a histogram of the first-passage time τ. For a system with ST [Fig. 2(a)] we notice that most of the particles hop, taking the first chance of low activation energy. This is in contrast with the system without ST [Fig. 2(b)], for which we observe many bumps of probability with the spacing $\tau_p=2\pi/\omega_0$ [12–14].

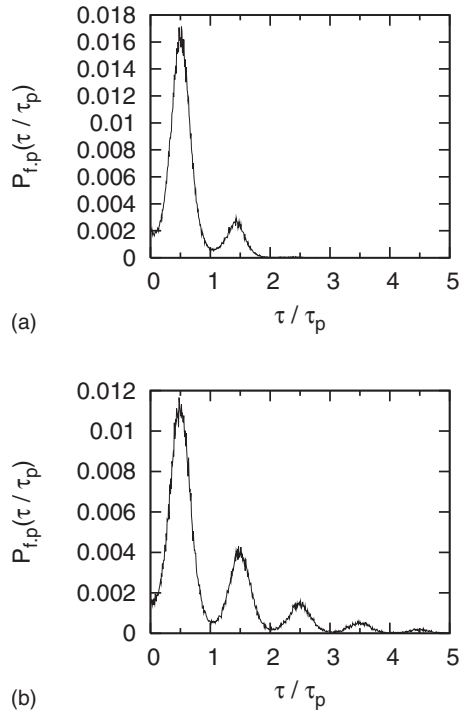

FIG. 2. First-passage time distribution functions for the system marked by a black circle (a) and by a white circle (b) in Fig. 1.

We discuss now the overall T dependence of the SNR shown in Fig. 1 based on the time-averaged activation energy [Fig. 3(a)], $\bar{a}=\tau_p^{-1}\int_0^{\tau_p}a(t)$ with $\tau_p\equiv2\pi/\omega_0$, and on a time-averaged firing rate fr similarly defined as $\bar{a}$ [Fig. 3(b)]. In the low-temperature region ($T<0.25$), the firing rate fr is increased since ST lowers the activation barrier $\bar{a}$ ($<a=0.5$). However, in the high-temperature region ($T>0.25$) where the noise intensity is high, the SNR is deteriorated by ST due to a considerable increase of $\bar{a}$, which results in a rapid decrease of fr compared with the fixed-threshold case [Fig. 3]. Firing events are in general useful for information transfer, and our results suggests that rapid growth of $\bar{a}$ as T increases is not welcome from the point of information processing by a threshold device. The behavior of $\bar{a}$ and fr depends on the parameters α and β in Eq. (6), and this will be considered in the next section.

Before proceeding to this problem, we show a typical example of Monte Carlo trajectories $(x(t),a(t))$ together with

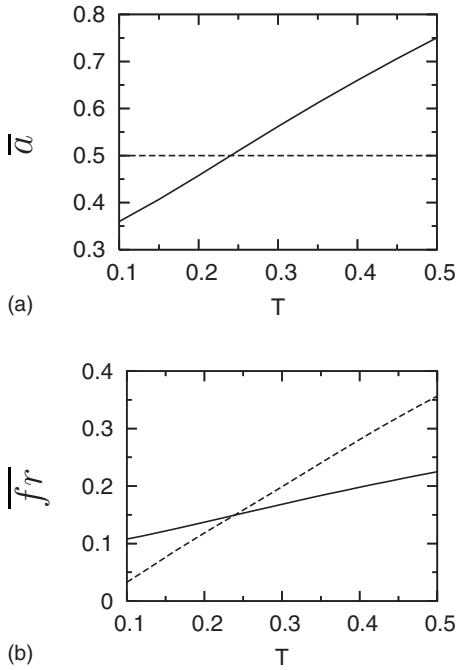

FIG. 3. Time-averaged activation energy $\bar{a}$ (a) and time-averaged firing rate $\overline{\text{fr}}$ as functions of T (b). Parameter values used for the solid and dashed curves correspond to the ones in Fig. 1.

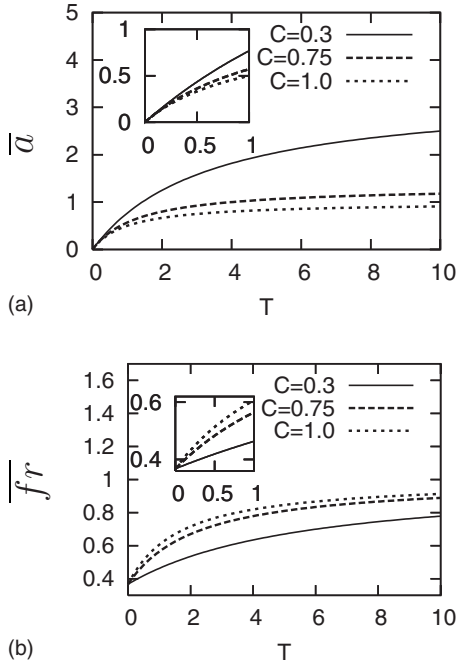

FIG. 5. Time-averaged activation energy $\bar{a}$ (a) and time-averaged firing rate $\overline{\text{fr}}$ (b) as functions of T from Eq. (19)

the input signal $A_0 \cos(\omega_0 t)$ in Fig. 4(a) for the system marked by solid squares (a) and open squares (b), belonging to the high-T region (T=0.4). When T and consequently

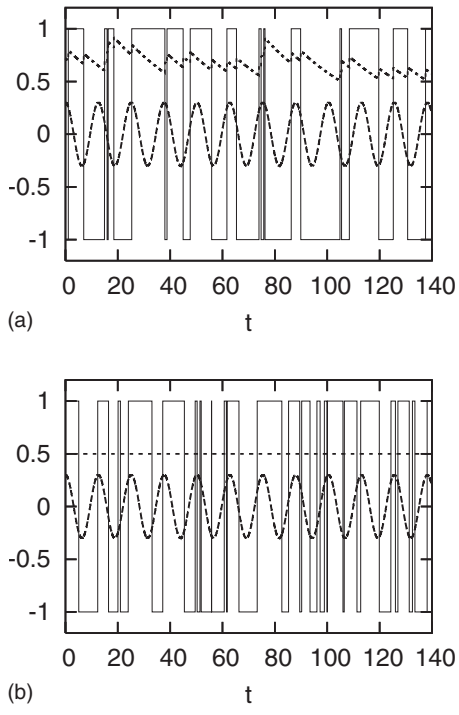

FIG. 4. Dynamical behavior $x(t)=\pm 1$ (solid curves) and $a(t)$ (dotted curves) from Monte Carlo simulations together with the sinusoidal signals $A_0 \cos(\omega_0 t)$ (dashed curves) for the system marked by the solid squares (a) and the open squares (b) in Fig. 1 with α=0.03 and β=0.1.

noise are large, we have some chances of successive hopping events as shown in Fig. 4. In this case the activation energy $a(t)$ increases rapidly as shown in Fig. 4(a) (typically around $t \simeq 80$) due to ST, which inhibits a firing event on average for some time. That is, in our Monte Carlo simulations we increase $a(t)$ by β whenever there occurs a hopping event [see Eq. (6)]. From this we intuitively see that large β values make $a(t)$ large, resulting in small fr(t). With these preparations we now consider the α and β dependence of SNR.

IV. THRESHOLD DYNAMICS AND SNR

Now let us consider Eq. (6), which describes the time evolution of the barrier height $a(t)$, and express it as

$$da/dt = -\alpha a(t) + \beta \,\text{fr}(t), \tag{18}$$

where fr(t) denotes the firing rate at time t. Since we are mainly interested in a subthreshold situation [i.e., $a(t) > A_0$] and the large-T region where ST did not work well compared

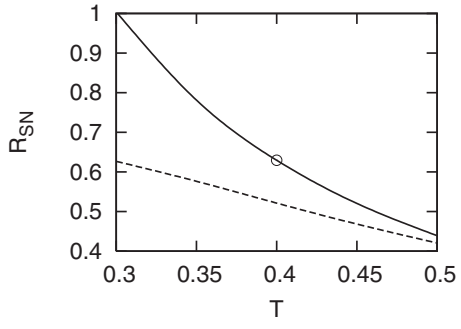

FIG. 6. SNR (R_{SN}) with ST (α=0.03, β=0.04, C=0.75) (solid curve) and without ST (dashed curve).

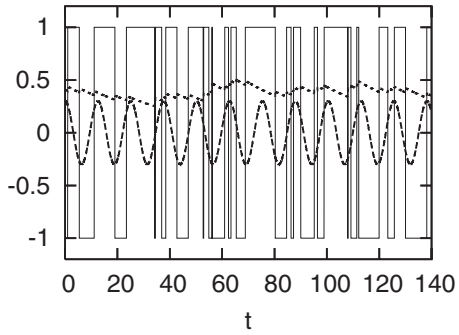

FIG. 7. Dynamical behavior $x(t)=\pm 1$ (solid curves) and $a(t)$ (dotted curves) from Monte Carlo simulations together with the sinusoidal signals $A_0\cos(\omega_0 t)$ (dashed curves) for the system marked by the open circle in Fig. 6.

with the weak-noise region (see Fig. 1), we neglect for qualitative discussion A_0/T in Eq. (2) and obtain, with the use of a simple form for the Kramers rate [4],

$$(\alpha/\beta)\bar{a} \equiv C\bar{a} = \exp(-\bar{a}/T), \tag{19}$$

after time averaging both sides of Eq. (18) for one period $\tau_p=2\pi/\omega_0$ of the external field. From this we see that at large T, $\bar{a}\to 1/C$ and $\bar{\text{fr}}\to[1-1/(TC)]$. In Fig. 5(a) we show $\bar{a}$ as a function of T, which is obtained by solving Eq. (19) for three values of $C\equiv\alpha/\beta$ ($C=0.3, 0.75, 1.0$ from above). We notice that the barrier height $\bar{a}$ remains small even for large T when $C\equiv\alpha/\beta$ becomes large. The firing rate $\bar{\text{fr}}$, calculated from Eqs. (2), (6), and (19), is shown in Fig. 5(b) ($C=0.3, 0.75, 1.0$ from below). Reflecting the fact that $\bar{a}$ does not increase rapidly with T when C is large, the firing rate seems to remain large in the large-T region when C becomes slightly larger than 0.3.

Guided by this observation we choose $C=0.75$ ($\alpha=0.03$ and $\beta=0.04$) and plot the SNR in Fig. 6 as a function of T. Compared with the solid curve in Fig. 1 we notice that the SNR is improved considerably and our ST seems to work well even in the high-T region by choosing proper values for $C=\alpha/\beta$.

Details of dynamics $(x(t), a(t))$ are shown in Fig. 7 for the system marked with an open circle in Fig. 6. This should be compared with the dynamics in Fig. 4(a) which is characterized by different parameter values ($\alpha=0.03$, $\beta=0.1$, $C=0.3$).

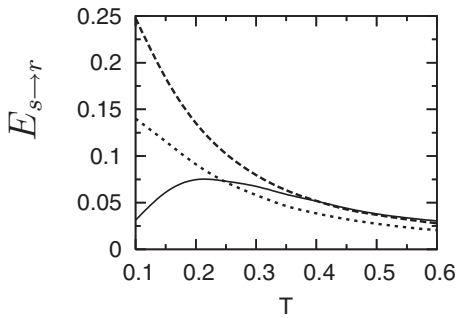

FIG. 8. Energy transfer rate $E_{s\to r}$ as a function of T for the system without ST (solid curve) and with ST with $\alpha=0.03$, $\beta=0.1$ (dotted curve) and $\alpha=0.03$, $\beta=0.04$ (dashed curve).

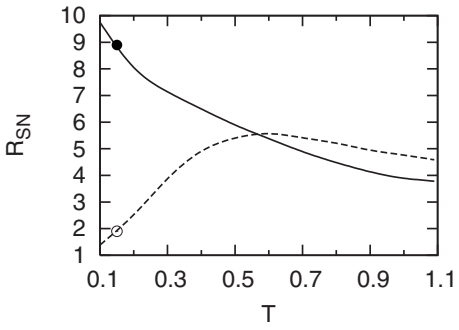

FIG. 9. SNR (R_{SN}) for the DWPS with ST (solid curve) and without ST (dashed curve). For ST we use $\alpha=0.05$, $\beta=0.05$ in Eq. (7) and the barrier height is set $a=1$ for the system without ST where $A_0=0.8$ and $\omega_0=0.5$.

By choosing a smaller value for β (=0.04) (keeping α fixed to 0.03) we could prevent the activation energy from becoming too large and this contributes to making the SNR large.

V. ENERGY TRANSFER, DWPS, AND CONCLUSION

In this section we consider briefly energy transfer from input signals to the reservoir (i.e., dissipation) and the DWPS, Eqs. (3)–(5), before concluding this paper.

The hopping rate, Eq. (6), can be rewritten as

$$w_+(t) = \exp\{-[V_s - V_1(t)]/T\},$$

$$w_-(t) = \exp\{-[V_s - V_{-1}(t)]/T\}, \tag{20}$$

with $V_s(=a)$ and $V_{\pm 1}(t)$ the energy at the saddle point ($x=0$) and at the position $x=\pm 1$, respectively. If $x(t)$ changes at

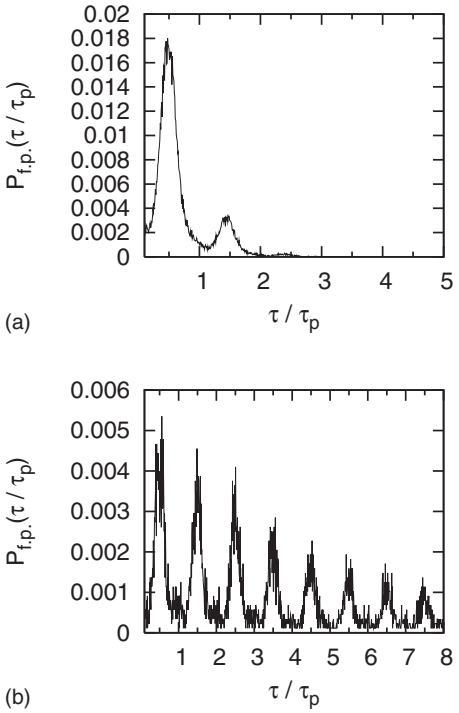

FIG. 10. First-passage time distribution function $p_{fp}(\tau/\tau_p)$ for the DWPS with ST (a) and without ST (b) at $T=0.15$. Parameter values characterizing the system are the same with those for Fig. 9.

$t=t_1$ from -1 to 1, the energy $\Delta E(t_1)$ transferred from the signal to the reservoir is given by $\Delta E=-[V_1(t_1)-V_{-1}(t_1)]=2V_{-1}(t_1)$. Dividing all the energy $\Sigma_i \Delta E(t_i)$ by the experimental duration τ_{expt} and $\bar{a}$, we have

$$E_{s\to r}=\sum_i \Delta E(t_i)/(\tau_{expt}\bar{a}), \tag{21}$$

which was obtained by Monte Carlo experiments.

In Fig. 8 is plotted $E_{s\to r}$ as a function of T. The dotted curve ($\alpha=0.03$, $\beta=0.04$), the dashed curve ($\alpha=0.03$, $\beta=0.1$), and the solid curve correspond to the systems represented by the solid curve in Fig. 6, the solid curve in Fig. 1, and the dashed curve in Fig. 1, respectively. We see that the SNR and $E_{s\to r}$ show surprisingly similar behaviors. This is rather natural since both quantities depend on the firing rate and the firing timing in similar ways. Especially the firing timing is important for both the SNR and $E_{s\to r}$. When a hopping event from $x=-1$ to $x=1$ occurs at time t_1, maximum energy transfer is achieved when V_{-1} becomes maximum at time t_1. This synchrony is evidently reflected to the SNR. As noted in Sec. I the synchrony is also important for SNR.

A final comment is on the double-well potential system, Eqs. (3)–(5). Since the TSS and DWPS describe similar hopping events under time periodic signals, we expect that both systems share common properties, especially in relation to ST and SR. Figure 9 shows the SNR of the DWPS with (solid curve) and without (dashed curve) ST, where the SNR is defined as the ratio $P(\omega_0)/[P(\omega_0-d\omega)/2+P(\omega+d\omega)/2]$ with $P(\omega)$ denoting the power spectral density at frequency ω and $d\omega$ is the frequency mesh size in numerical calculations of $P(\omega)$. This should be compared with Fig. 1 for the TSS. Corresponding to Fig. 2, we compare $p_{fp}(\tau)$ for the two systems marked by an open and solid circle in Fig. 9 in Fig. 10. From these results it is seen that the TSS and DWPS behave similarly with respect to response to and information transfer of the periodic signals.

In this paper we applied a ST mechanism, Eq. (6), to the TSS, Eq. (1), and confirmed that a better SNR is simply obtained by the ST mechanism for the small-fluctuation (i.e., low-T) region. Tuning of the parameters α and β was guided by a simple equation (19), leading to a better SNR even for the high-T region. The energy transfer or dissipation rate was also studied, and this quantity (21) turned out to be able to play a similar role as a measure of the information processing ability of a threshold device.

[1] V. S. Anishchenko, V. V. Astakhov, A. B. Neiman, T. E. Vadivasova, and L. Schimansky-Geier, *Nonlinear Dynamics of Chaotic and Stochastic Systems* (Springer, Berlin, 2002); L. Gammaitoni, P. Hänggi, P. Jung, and F. Marchesoni, Rev. Mod. Phys. **70**, 223 (1998).

[2] P. Reimann, Phys. Rep. **361**, 57 (2002); F. Jülicher, A. Ajdari, and J. Prost, Rev. Mod. Phys. **69**, 1269 (1997).

[3] S. Kirkpatrick, C. D. Gelatt, and M. P. Vecchi, Science **220**, 671 (1983).

[4] H. A. Kramers, Physica (Amsterdam) **7**, 284 (1940); S. Chandrasekhar, Rev. Mod. Phys. **15**, 1 (1943); in *Selected Papers on Noise and Stochastic Processes*, edited by N. Wax (Dover, New York, 1954).

[5] A. K. Hartmann and H. Rieger, *Optimization Algorithms in Physics* (Wiley-VCH, Berlin, 2002).

[6] F. Marchesoni, F. Apostolico, and S. Santucci, Phys. Rev. E **59**, 3958 (1999); F. Apostolico, L. Gammaitoni, F. Marchesoni, and S. Santucci, *ibid.* **55**, 36 (1997).

[7] R. Benzi, S. Sutera, and A. Vulpiani, J. Phys. A **14**, L453 (1981).

[8] A. B. Neiman, D. F. Russel, X. Pei, W. Wojtenek, J. Twitty, E. Simonotto, B. A. Wetting, E. Wagner, L. A. Wilkens, and F. Moss, Int. J. Bifurcation Chaos Appl. Sci. Eng. **10**, 2499 (2000).

[9] T. Munakata, T. Hada, and M. Ueda, Physica A **375**, 492 (2007).

[10] W. Denk, W. W. Webb, and A. J. Hudspeth, Proc. Natl. Acad. Sci. U.S.A. **86**, 5371 (1989); S. Camalet, T. Duke, F. Jülicher, and J. Prost, *ibid.* **97**, 3183 (2000).

[11] B. McNamara and K. Wiesenfeld, Phys. Rev. A **39**, 4854 (1989).

[12] T. Zhou, F. Moss, and P. Jung, Phys. Rev. A **42**, 3161 (1990).

[13] L. Gammaitoni, F. Marchesoni, E. Menichella-Saetta, and S. Santucci, Phys. Rev. Lett. **62**, 349 (1989).

[14] L. Gammaitoni, F. Marchesoni, and S. Santucci, Phys. Rev. Lett. **74**, 1052 (1995).